Field-Plate Optimization of AlGaN/GaN HEMTs

Vassil Palankovski*, Stanislav Vitanov*, and Rüdiger Quay†
*Advanced Materials and Device Analysis Group, Inst. for Microelectronics, TU Wien, Gußhausstr. 27–29, 1040 Wien, Austria
Email: {palankovski,vitanov}@iue.tuwien.ac.at
†Fraunhofer Inst. for Solid-State Physics (IAF), Tullastr. 72, 79108 Freiburg, Germany
Email: ruediger.quay@iaf.fraunhofer.de

Abstract— **An investigation on the field plate technique in AlGaN/GaN power HEMTs is presented. The critical geometrical variables controlling the field distribution in the channel are determined and optimized for improved device reliability using two-dimensional numerical simulations. The results are implemented in the design of devices fabricated with 600 nm down to 150 nm gate lengths. Good agreement between experimental and simulation data is achieved.**

I. Introduction

Wide bandgap GaN-based high electron mobility transistors (HEMTs) have demonstrated impressive power capabilities in radio frequency range. Since their description in 1993 [1] they have reached power densities exceeding 10 W/mm in recent years [2]–[4]. Thus, AlGaN/GaN devices have established themselves as microwave power devices. A significant improvement of the device performance has been achieved by adopting the field plate technique [5]. With its origins in the context of high-voltage p-n junctions [6] the main functions of the field plate are to reshape the electric field distribution in the channel and to reduce its peak value on the drain side of the gate edge. The benefit is an increase of the breakdown voltage and a reduced high-field trapping effect. Overall the power density could be increased from 10 W/mm [7] to 40 W/mm [8]. Although sharing the same principle with FETs/MESFETs the effect of the field plate on HEMTs has to be studied extensively with account of the different transport mechanisms in the later devices. In HEMTs the polarization charge at the AlGaN/GaN heterointerface is the crucial factor building the channel. In this work, the electric field distribution in the channel is optimized by variation of the geometry of the field plate using the two-dimensional device simulator MINIMOS-NT [9]. While other work [10] discusses a setup with the field plate electrically connected to the source contact, our research addresses the case of a field plate connected to the gate.

II. Device Structure and Fabrication

The AlGaN/GaN HEMT technology is based on multi-wafer MOCVD growth on 2-inch semi-insulating SiC substrates based on an Aixtron 2000 multi-wafer reactor. The gate is so far e-beam defined with a gate length of l_{g}=150 nm, 300 nm, and 600 nm. Device isolation is achieved by mesa isolation. Fig. 1 gives an example of a typical fully planar AlGaN/GaN HEMT field-plated structure. An $\mathrm{Al_{0.3}Ga_{0.7}N}$/GaN heterointerface is grown on top of a thick insulating GaN buffer. All layers are non-intentionally doped, except the δ-doping which is introduced in the AlGaN supply layer to provide additional carriers and to improve the access resistances. The maximum drain current density is larger than 900 mA/mm and the transconductance is larger than 200 mS/mm at V_{DS}=7 V. The current gain cut-off frequency f_{T} is well beyond 30 GHz for devices with l_{g}=300 nm.

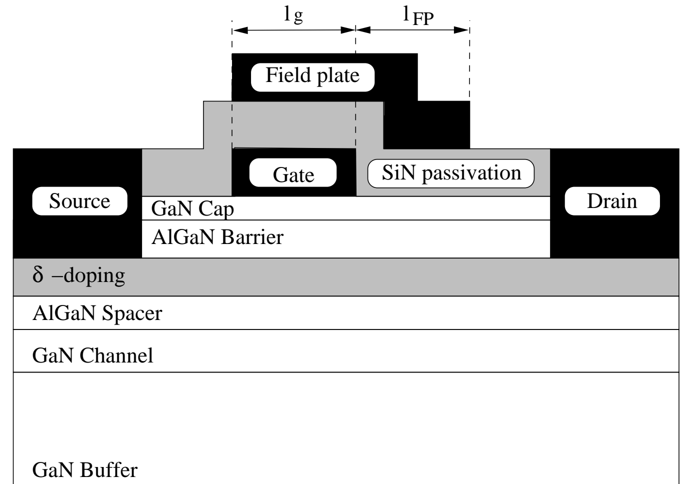

Fig. 1. A schematic layer structure of single heterojunction AlGaN/GaN HEMTs with field plates investigated in this work.

III. Simulation Setup

The physical models for GaN-based materials from [11] have been implemented in MINIMOS-NT which is a suitable tool for analysis of heterostructure devices [12].

We study the penetration depth of the drain/source metal contacts which build an alloy with the AlGaN supply layer. While it has a major influence on the electrical characteristics of the device its impact on the electrical field distribution in the channel is found to be negligible. In our calibrated setup a metal diffusion prolonging to the δ-doping layer is adopted.

Since the longitudinal electric field in the channel reaches peak values of above 500 kV/cm, a hydrodynamic approach is used to properly model electron transport and energy relaxation. A low-field electron mobility model is fitted to own Monte Carlo simulation results [13]. We consider electron energy relaxation times which depend on electron energy and lattice temperature. Fig. 2 compares our analytical model to Monte Carlo simulation data for GaN.

We further assess the impact of thermionic emission and field emission (tunneling) effects which critically determine

1-4244-0126-7/06/$20.00©2006 IEEE.

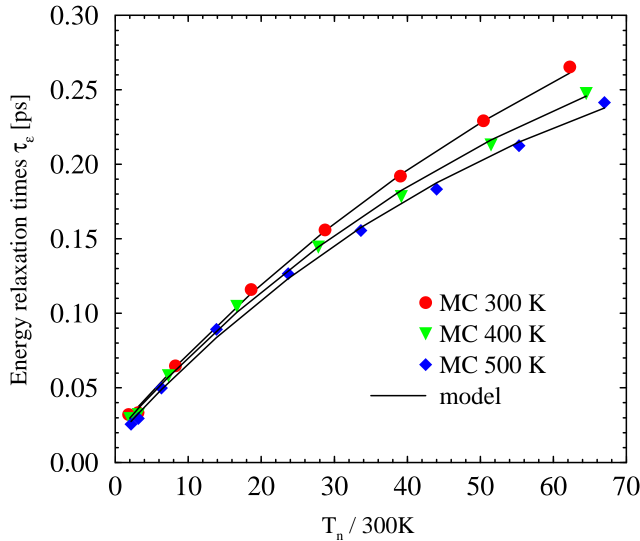

Fig. 2. Electron energy relaxation times as a function of electron temperature for different lattice temperatures

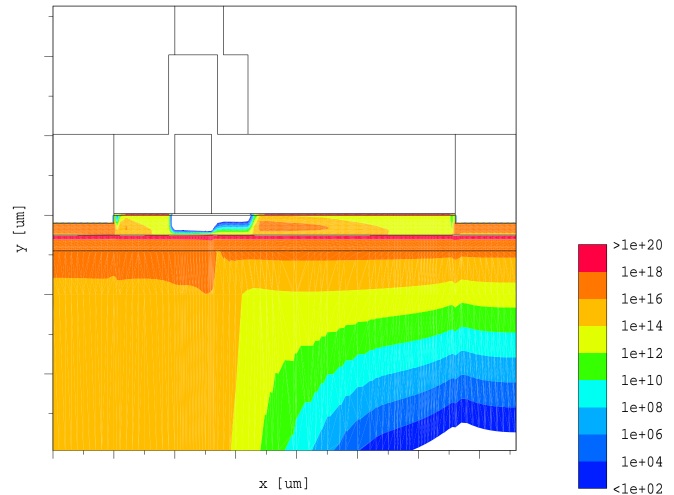

Fig. 4. Simulated electron concentration (given in [cm^{-3}]) in an AlGaN/GaN HEMT with l_g=l_{FP}=600 nm for V_{GS}=0 V and V_{DS}=7 V.

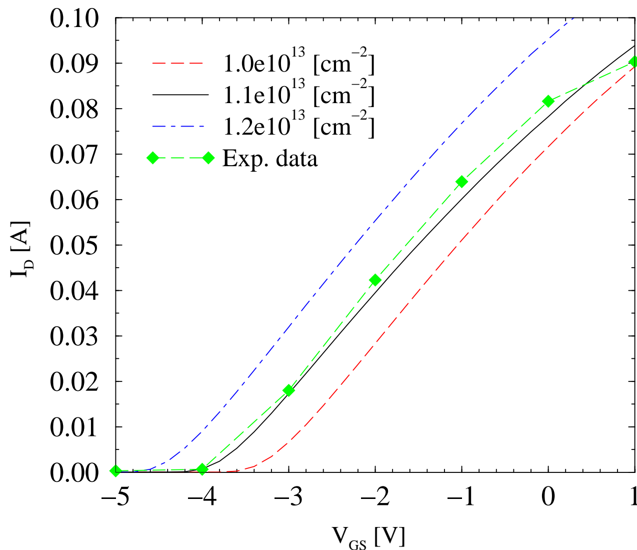

Fig. 3. Transfer characteristics for different polarization charge densities at the AlGaN/GaN heterojunctions.

the current transport across the heterojunctions. An optimal tunnel length of 7.5 nm is found. Self-heating (SH) effects are accounted for by using a global temperature model.

In order to properly describe the two-dimensional electron gas in the channel, the value of the positive polarization charge density [14] at the GaN-channel/AlGaN-spacer interface is assessed. This positive charge is compensated by a negative surface charge at the AlGaN-barrier/GaN-cap interface and at the bottom of the buffer. The density is found to be $\approx 1.1\times10^{13}cm^{-2}$ (see Fig. 3). An energy barrier height of 1 eV at the Schottky gate contact is assumed. As can be seen in Fig. 4 (the electron concentration for V_{DS}=7 V, V_{GS}=0 V is shown) the device is a normally on transistor.

IV. Simulation Results

The critical variables associated with the field plate for a given gate length l_g are the field plate length l_{FP} and the SiN thickness (see Fig. 1). While the gate length is crucial for the transit time, the field plate length is the major factor for the size of the electrical field-reshaped region. The nitride thickness controls the onset voltage but has also a significant influence on the maximum electric field.

A. Calibration and Field Plate Optimization of l_g=600 nm HEMTs

AlGaN/GaN HEMTs with l_g=600 nm have been used for device analysis and model calibration. A concise set of models and model parameters has been obtained first for devices without field plates [13]. This set is applied here also to field-plated HEMTs. Fig. 5 shows measured (solid lines) and simulated (dashed lines) output characteristics of l_g=l_{FP}=600 nm HEMTs. Modeling issues remain for V_{GS}=1 V. Fig. 6 compares measured (symbols) and simulated (lines) transfer characteristics of HEMTs without and with field plate. Very good agreement between simulation and measured electrical data is achieved for both devices. The difference caused by the field plate is better demonstrated by the electrical field distribution in the channel as shown in Fig. 7. A 50% reduction of the maximum electric field, located at the drain side of the gate edge, is achieved by the introduction of the field plate. A second peak occurs at the field plate edge.

The choice of an optimum field plate length is made with respect to the desired electrical properties [15]. In this work, we aim at highest reduction of the peak electric fields in the channel for V_{GS}=V_{FPS}=−7 V, V_{DS}=60 V, thus securing a reliable device operation up to this bias. The optimum field plate length l_{FP}=l_g=600 nm is found after variation of l_{FP} in the range 200 nm-800 nm (see Fig. 8).

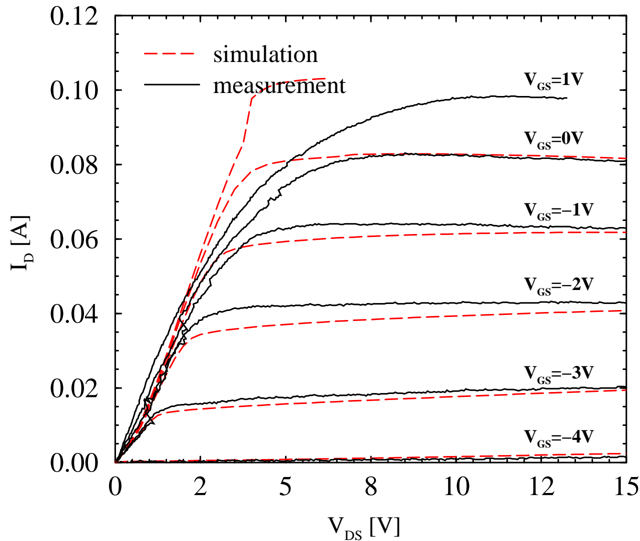

Fig. 5. Comparison of measured (solid lines) and simulated (dashed lines) output characteristics of $l_{\rm g}$=$l_{\rm FP}$=600 nm HEMTs.

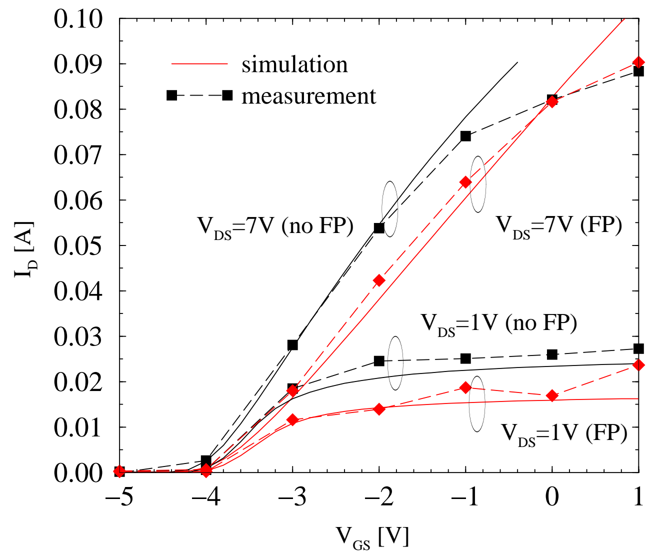

Fig. 6. Comparison of measured (symbols) and simulated (lines) transfer characteristics of HEMTs with and without field plate.

B. Field Plate Optimization of Shorter HEMTs

Fig. 9 shows simulation results for HEMTs with shorter gate lengths down to 150 nm. While such devices are economically favored, our results show that for small $l_{\rm g}$ the maximum electric field increases by up to 60%, thus requiring a mechanism to compensate the negative impact. The field plate length is kept equal to $l_{\rm g}$. The optimum value for the thickness of the nitride passivation in $l_{\rm g}$=600 nm devices is further preserved.

Our next simulations sets involve devices with $l_{\rm g}$=300 nm (Fig. 10). Increasing $l_{\rm FP}$ is advantageous up to $l_{\rm FP}$=500 nm regarding the peak electrical field. Fig. 11 shows electrical field distribution in the channel of $l_{\rm g}$=150 nm HEMTs. $l_{\rm FP}$ varies from 100 nm to 400 nm. Compared with the previous simulations a clear improvement for longer field plates is observed. The increase of $l_{\rm FP}$ from 150 nm to the optimum of about 350 nm helps to decrease the peak electrical field by up to 40%.

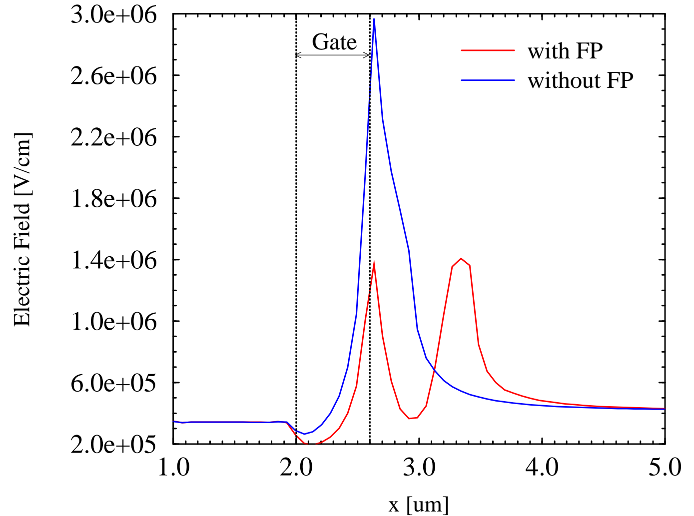

Fig. 7. Simulated electric field along the channel of $l_{\rm g}$=600 nm HEMTs with and without field plate for $V_{\rm GS}$=0 V and $V_{\rm DS}$=7 V.

V. Conclusion

Our two-dimensional device simulator is extended to GaN-based materials. It is calibrated using experimental data from HEMTs and subsequently employed in an investigation and optimization of the field plate technique, which seems promising for enhancement of the breakdown voltage. The approach is applied to devices with various gate lengths. The peak electric field is reduced by $40\% - 50\%$. The simulation results show that the optimum field-plate lengths do not scale as much as the gate lengths.

Acknowledgment

Support by the Austrian Science Funds FWF and BMWK, START Project No.Y247-N13, and by the TARGET European Network of Excellence is acknowledged.

References

[1] M.A. Khan, A. Bhattarai, J.N. Kuznia, and D.T. Olson, "High Electron Mobility Transistor Based on a GaN-Al$_x$Ga$_{1-x}$N Heterojunction," *Appl. Phys. Lett.*, vol. 63, pp. 1214–1215, Aug. 1993.

[2] Y.F. Wu, B.P. Keller, P. Fini, S. Keller, T.J. Jenkins, L.T. Kehias, S.P. Dnebaars, and U.K. Mishra, "High Al-Content AlGaN/GaN MODFET's for Ultrahigh Performance," *IEEE Electron Dev. Lett.*, vol. 19, pp. 50–53, Feb. 1998.

[3] V. Tilak, B. Green, V. Kaper, H. Kim, T. Prunty, J. Smart, J. Shealy, and L. Eastman, "Influence of Barrier Thickness on the High-Power Performance of AlGaN/GaN HEMTs," *IEEE Electron Dev. Lett.*, vol. 22, pp. 504–506, Nov. 2001.

[4] A. Chini, D. Buttari, R. Coffie, L. Shen, S. Heikman, A. Chakraborty, S. Keller, and U.K. Mishra, "High Performance AlGaN/GaN HEMTs with a Field Plated Gate Structure," in *Proc. IEEE Intl. Semiconductor Device Research Symp.*, Washington, USA, Dec. 2003, pp. 434–439.

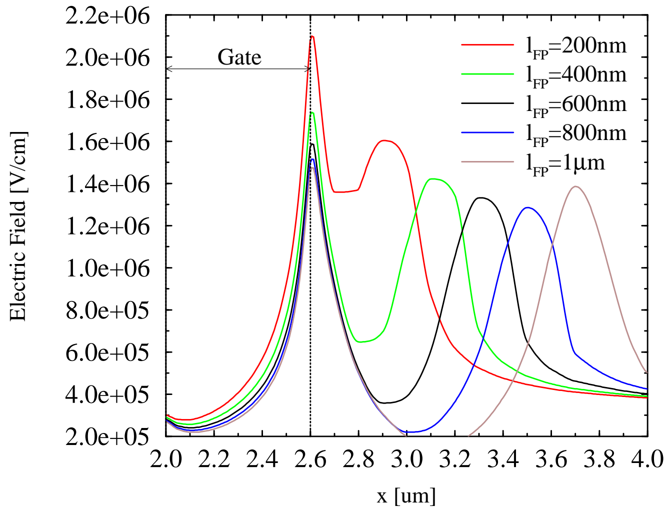

Fig. 8. Simulated electric field along the channel for various field plate lengths l_{FP} (l_{g}=600 nm).

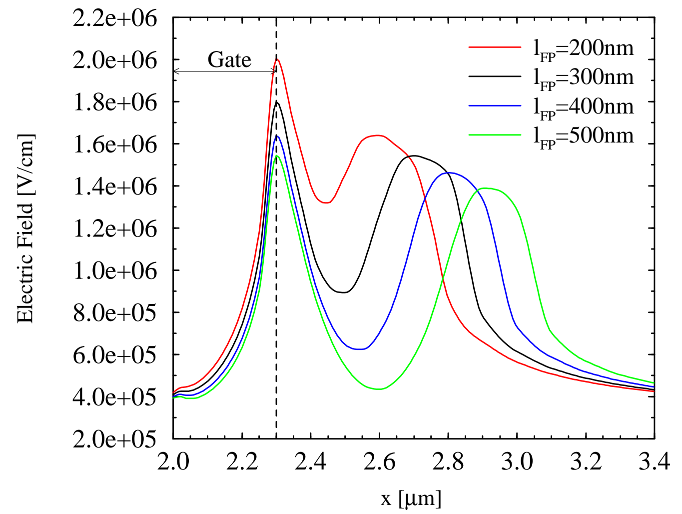

Fig. 10. Simulated electric field along the channel for various field plate lengths l_{FP} (l_{g}=300 nm).

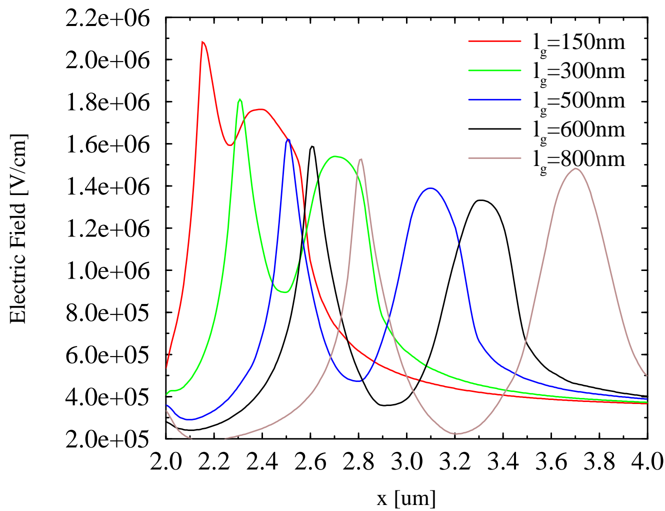

Fig. 9. Simulated electric field along the channel for various gate lengths (l_{FP}=l_{g}).

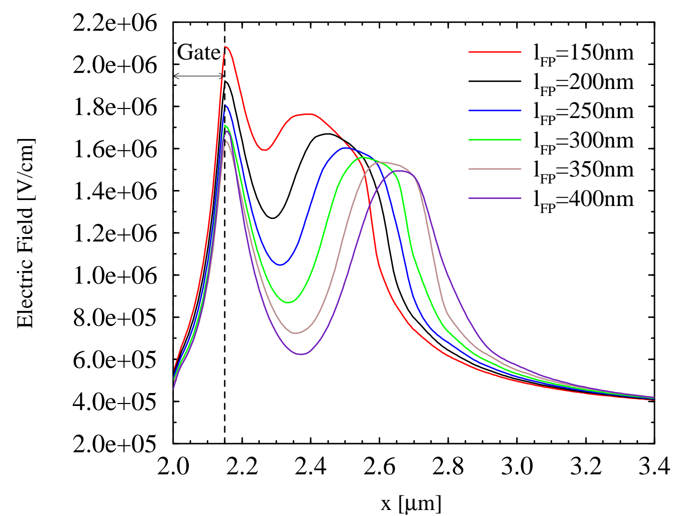

Fig. 11. Simulated electric field along the channel for various field plate lengths l_{FP} (l_{g}=150 nm).

[5] N.Q. Zhang, S. Keller, G. Parish, S. Heikman, S.P. Denbaars, and U.K. Mishra, "High Breakdown in GaN HEMT with Overlapping Gate Structure," *IEEE Electron Dev. Lett.*, vol. 21, pp. 421–423, Sept. 2000.

[6] F. Conti and M. Conti, "Surface Breakdown in Silicon Planar Diodes Equipped with a Field Plate," *Solid State Electron.*, vol. 15, pp. 93–105, Jan. 1972.

[7] Y. Ando, Y. Okamoto, H. Miyamoto, T. Nakayama, T. Inoue, and M. Kuzuhara, "10-W/mm AlGaN-GaN HFET with a Field Modulating Plate," *IEEE Electron Device Lett.*, vol. 24, pp. 289–291, May 2003.

[8] Y.-F. Wu, M. Moore, A. Saxler, M. Moore, T. Wisleder, and P. Parikh, "40-W/mm Double Field-plated GaN HEMTs," in *Proc. 64th IEEE Dev.Res.Conf.*, State College, PA, USA, June 2006, (in print).

[9] Institut für Mikroelektronik, Technische Universität Wien. (2002) Minimos-NT Device and Circuit Simulator, User's Guide, Release 2.0. Available: http://www.iue.tuwien.ac.at/software/minimos-nt

[10] W. Saito, Y. Takada, M. Kuraguchi, K. Tsuda, I. Omura, T. Ogura, and H. Ohashi, "High Breakdown Voltage AlGaN-GaN Power-HEMT Design and High Current Density Switching Behaviour," *IEEE Trans. Electron Dev.*, vol. 50, pp. 2528–2531, Dec. 2003.

[11] V. Palankovski and R. Quay, *Analysis and Simulation of Heterostructure Devices*. Wien, New York: Springer, 2004.

[12] V. Palankovski, R. Quay, and S. Selberherr, "Industrial Application of Heterostructure Device Simulation," *IEEE J. Solid-State Circuits*, vol. 36, no. 9, pp. 1365–1370, (invited), Sept. 2001.

[13] S. Vitanov, V. Palankovski, R. Quay, and E. Langer, "Modeling of Electron Transport in GaN-Based Materials and Devices," in *Proc. Intl. Conf. on Physics of Semiconductors*, Vienna, Auistria, July 2006, (in print).

[14] O. Ambacher, B. Foutz, J. Smart, J. Shealy, N. Weinman, K. Chu, M. Murphy, A. Sierakowski, W. Schaff, L. Eastman, R. Dimitrov, A. Mitchell, and M. Stutzman, "Two-Dimensional Electron Gases Induced by Spontaneous and Piezolectric Polarization in Undoped and Doped AlGaN/GaN Heterostructures," *J. Appl. Phys.*, vol. 87, pp. 334–344, Jan. 2000.

[15] S. Karmalkar and U.K. Mishra, "Enhancement of Breakdown Voltage in AlGaN/GaN High Mobility Transistors Using a Field Plate," *IEEE Trans. Electron Dev.*, vol. 48, pp. 1515–1521, Aug. 2001.